Peer-reviewed version available at Appl. Sci. 2018, 8, 278; doi:10.3390/app8020278

Article

Bio-Inspired Optimal Control Framework to Generate Walking Motions for the Humanoid Robot iCub Using Whole Body Models

Yue Hu [1,*] and Katja Mombaur [1]

1 Optimization, Robotics & Biomechanics, Institute of Computer Engineering, Heidelberg University, Berliner Str. 45, 69120 Heidelberg, Germany; {yue.hu,katja.mombaur}@ziti.uni-heidelberg.de

* Correspondence: yue.hu@ziti.uni-heidelberg.de

Abstract: Bipedal locomotion remains one of the major open challenges of humanoid robotics. The common approaches are based on simple reduced model dynamics to generate walking trajectories, often neglecting the whole-body dynamics of the robots. As motions in nature are often considered as optimal with respect to certain criteria, in this work we present an optimal control based approach that allows us to generate optimized walking motions using a precise whole-body dynamic model of the robot, in contrast with the common approaches. The optimal control problem is formulated to minimize a set of desired objective functions with respect to physical constraints of the robot and contact constraints of the walking phases. We apply the method with combinations of different objective criteria to the model of a reduced version of the iCub humanoid robot of 15 internal DOF. The obtained trajectories are executed on the real robot and we carry out a discussion on the differences between the outcomes of this approach with the classic approaches.

Keywords: humanoid robot; bipedal locomotion; optimal control; optimization

1. Introduction

Humanoid robots have been designed and built for decades, inspired by nature and in particular the human structure and behaviour. The goal is to use humanoid robots in environments that are made for and populated by humans, either supporting the human in his activities if they are too heavy or too boring, or replacing him in situations that are too dangerous. Also replacing the humans for work in space is a common target for humanoid robotics. Therefore, there is a general expectation that humanoid robots should be able to perform the same tasks and have the same motion capabilities as humans, and in the future even outperform humans in these tasks.

Ever since the first appearance of humanoid robots, many of them have been equipped with legs. However, bipedal locomotion capabilities of these robots are still far behind what humans are able to perform. Up to date, walking remains one of the major open challenges of bipedal humanoid robotics. The difficulty of achieving stable, dynamic and versatile walking for bipedal robots has many reasons: the anthropomorphic shape of the humanoid robot exhibits a high redundancy with respect to most motion tasks, but at the same time it is also difficult to determine feasible solutions, since many of the joint angle combinations result in infeasible motions. Humanoids are generally underactuated with no direct actuators for the overall position and orientation in space which have to be moved instead by a coordinated action of many other actuators considering feasibility. It should be noted that for most current humanoid robots, a typical human walking behaviour is much too challenging in terms of speed, joint motion ranges, required torques and impacts. Humanoid locomotion also involves changing contacts with the environment which have to be properly chosen. Stability control of humanoid locomotion is one of the biggest problems, since bio-inspired bipedal walking can not be performed in a statically stable way but must be dynamically stable. The precise definition of dynamic stability of human walking is still unknown, and up to now many humanoid robots still apply the well

Peer-reviewed version available at Appl. Sci. 2018, 8, 278; doi:10.3390/app8020278

known Zero Moment Point (ZMP) criterion [1] instead, which is very convenient to use but results in more conservative gaits.

Motion generation for humanoid robots can be divided in two main categories: motion remapping and model based generation.

In the first case, walking motions from humans are recorded via motion capturing systems, then they can be transferred to the robot by taking into account robot specific constraints such as physical constraints and stability criteria. The recorded motions can be first processed as motion primitives and then concatenated to generate complex motions, such as achieved on the robot HRP2 (Kawada) [2] or directly transferred to the robot by means of reduced models and adjustments of end effector positions as achieved on the JAXON robot [3].

In the case of model based motion generation, the most common method is to use reduced models together with the ZMP criterion. Reduced models are for example the Linear Inverted Pendulum (LIPM) [4] or the table cart [5], which allowed many robots to achieve stable walking, such as on HRP2 [6] by means of NonLinear Model Predictive Control (NMPC), on the compliant humanoid robot CoMan [7] and iCub [8]. In all these cases the whole-body posture is computed by means of Inverse Kinematics matching the desired end effector positions computed with the dynamics of the reduced models. The main reason for which reduced models are up to date widely used is because they allow for fast online control. However it is known that due to the many assumptions that are introduced due to the use of such models, the whole-body dynamics of the robot is not well-exploited and the motions often appear over-constrained and not very natural.

Another, more bio-inspired way of motion generation is to use optimization, or to be more precise optimal control, based on whole body models of the robots. Optimality is often considered to be a guiding principle of nature, and movements which are performed frequently such as everyday motions or trained motions, tend to be optimal with respect to some optimality criterion. By the use of mathematical optimization in the generation of motions for humanoid robots, this biological optimization process is mimicked. The optimization criteria used can be either biologically inspired or technically motivated. In addition, optimization helps to solve the feasibility and the redundancy issues of walking. It generates motions that are feasible with respect to all constraints that can be formulated in a detailed whole-body model of the robot and of the motion task. From all redundant solutions of a particular task, it selects the one that is optimal with respect to the chosen optimization criterion.

Optimal control has previously been used to generate challenging motions using whole-body models for robots such as HRP-2 [9–15]. In an approach which is situated between whole-body optimization and motion generation by reduced models, optimization of template models has been used for generating walking motion of humanoid robots in challenging scenarios [16].

In previous works we have achieved the first walking motions on one of the widest spread complex humanoid robots iCub [17], by means of the table cart model and ZMP criterion [8], allowing the robot to achieve walking on level ground, and for the first time, on slopes and stairs, with the aim of measuring the walking capabilities of iCub. In particular, this work has been performed on the reduced version of the iCub available in our lab with nor head and arms (named the HeiCub), but the results are transferrable to the full iCub models. We later improved the walking performances by means of a closed-loop control scheme based on NMPC, which allowed the robot to be able to change walking directions online [18].

In this work, instead, we want to use the whole-body dynamic model of the robot to generate walking motions on level ground. Similar to the setup of the problem for HRP-2 in [12], here we formulate the optimal control problem for walking using the detailed model of the the humanoid robot iCub / HeiCub. In the optimal control problem we set several objective functions and constraints to describe the hybrid dynamics of walking and to respect the physical constraints of the robot itself. The obtained motions are then transferred to the robot and the outcomes are discussed with a comparison with the motions we had previously achieved on the same robot with reduced models.

Preprints (www.preprints.org) | NOT PEER-REVIEWED | Posted: 15 December 2017 doi:10.20944/preprints201712.0099.v1

Peer-reviewed version available at Appl. Sci. 2018, 8, 278; doi:10.3390/app8020278

This paper is organized as follows: in 2 we give a description of the iCub humanoid robot and its reduced version HeiCub. Section 3 describes in detail the different walking phases involved in the optimal control problem as well as the dynamics equations in all cases. In 4 we illustrate the optimal control problem formulation giving the details of states, controls, parameters, objective functions, and constraints. Section 5 shows the numerical results, followed by the experimental results obtained on the robot in section 6. The paper concludes in section 7 with a final discussion on the work and conclusions as well as possible future developments.

2. The (He)iCub humanoid robot

The iCub [17] is a humanoid robot designed and built by the Fondazione Istituto Italiano di Tecnologia (IIT) and distributed among more than 30 research institutions and universities all over the world. The robot was originally designed with the aim of conducting cognitive studies, therefore it was meant to resemble a 3-to-4 years old child. The latest version of the robot consists of a whole-body humanoid with head, arms and legs, for a total of 53 degrees of freedom (DOF), including dexterous hands.

The iCub is mostly known for its grasping [19,20] and balancing [21] capabilities, which have been widely exploited by several works in past and recent years, while in the first versions of iCub the robot legs had weak actuators and small feet that did not allow the robot to perform walking but only crawling. In the last available version, the legs have been redesigned [22] inspired by the mechanical design of the CoMan humanoid robot, which has demonstrated several walking capabilities [23–25].

In the context of the European Project KoroiBot, IIT has delivered to Heidelberg University a reduced version of the standard iCub, consisting of 15 internal DOF: 3 in the torso and 6 in each leg, as shown in Fig. 1. The robot is furthermore equipped with 4 force torque sensors (F/T), two in the upper legs and two in the feet. The robot has an on-board PC104 with dual core, but has no battery, therefore it needs to be connected to external power suppliers by means of cables, which serve also as network communication cables, allowing to use external computers to carry out bulky computations. The robot has also 4 custom Series Elastic Actuators (SEA) [26] with springs that can be unmounted to obtain rigid actuators. In the context of this paper, the springs are unmounted and therefore the joints are considered perfectly rigid.

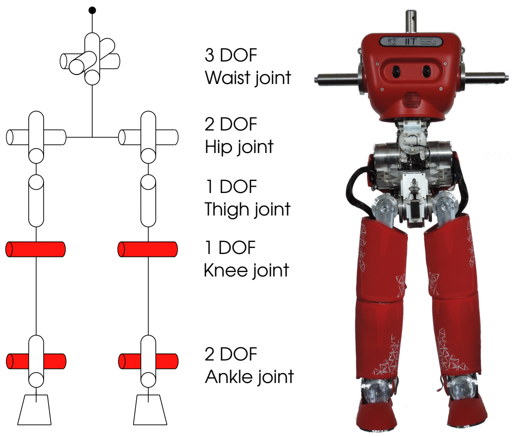

Figure 1. The HeiCub humanoid robot. In red the Series Elastic Actuators, which are not considered in the context of this work.

The robot has a weight of 26.4 [kg] and it is 0.97 [m] tall. The leg length (from the hip axis) is of 0.51 [m], and the feet are 0.2 [m] long and 0.1 [m] wide. The weight distribution of the robot is of about 6 [kg] for the torso, 5 [kg] for the pelvis and 7.5 [kg] each leg. All the kinematic and dynamic parameters of the robot are described in an URDF (Unified Robot Description Format) file which was extracted directly from the original CAD model.

Peer-reviewed version available at Appl. Sci. 2018, 8, 278; doi:10.3390/app8020278

To distinguish this robot from the standard iCub, we will use the name HeiCub (iCub of Heidelberg University) to refer to it from now on. The legs of HeiCub have the exact same mechanical design as any other standard iCub and uses also the same software infrastructure as the iCub. These features allow us to transfer control frameworks developed for the iCub to HeiCub and vice-versa, by just adapting the number of DOF and the upper body structure.

3. Model and Dynamics

As during walking different contacts are involved, we define walking as a hybrid dynamics system, where the dynamics switches according to contact conditions, i.e. hybrid and non-smooth dynamics. To have a precise description of the dynamics of walking, in the following we first list the phases that involve the different contacts and then the dynamics equations that will be used in the optimal control problem.

3.1. Walking phases

Different phases can be identified for a walking sequence. This is usually done also for human walking motions analysis [27], where the different feet contacts are described and the phases might change according to walking environment [28]. Differently from humans, HeiCub has a rigid flat foot, common among humanoid robots. Therefore, the walking phases for such a humanoid are different from human walking, as we have to consider completely flat contacts between the feet and the ground.

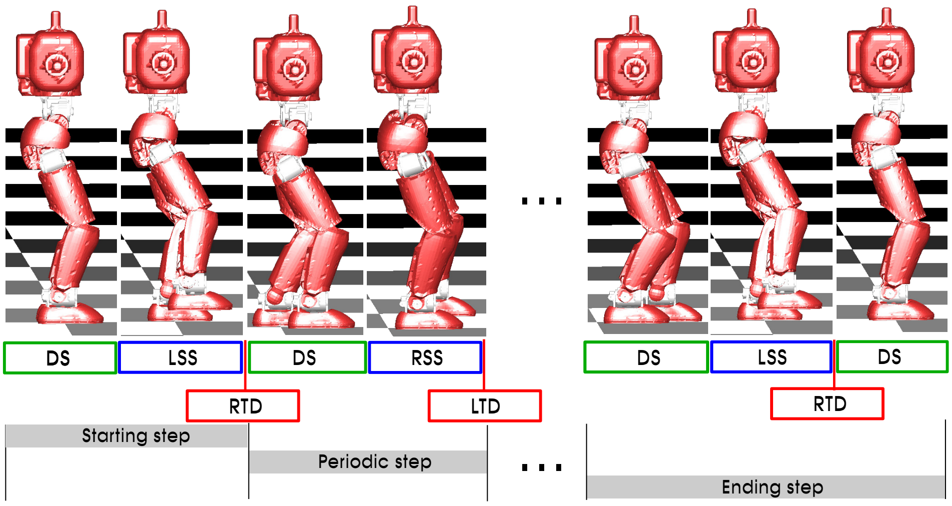

Figure 2. Walking phases of HeiCub. Where DS=Double Support, LSS=Left Single Support, RSS=Right Single Support, LTD=Left Touch Down, RTD=Right Touch Down. The whole sequence can be seen as three sub-sequences. The periodic step can be repeated for a desired number of times that do not need to be further modeled.

As shown in Fig. 2, the walking sequence can be seen as three sub-sequences:

- Starting step, the robot starts from a complete stop (i.e. all velocities to 0) and takes the first step, leading to the periodic motion.
- Periodic steps, which are the steps that the robot can repeat during the walking. In this case we assume single-step periodic, i.e. the left and right leg configurations can be mirrored, as the robot is symmetric.
- Ending step, the final step where the robot comes to a complete stop from the periodic motion.

It is to be noted that in this case we assume that one step is enough to lead the motion into a periodic motion and to lead the motion to an end. This assumption might not be valid for any system and

Preprints (www.preprints.org) | NOT PEER-REVIEWED | Posted: 15 December 2017 doi:10.20944/preprints201712.0099.v1

Peer-reviewed version available at Appl. Sci. 2018, 8, 278; doi:10.3390/app8020278

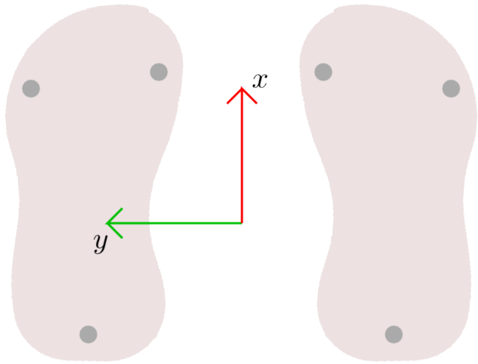

Figure 3. Feet shapes of the HeiCub robot. Three points are defined for contact modeling on each foot.

situation, however we have verified that in the cases we considered for HeiCub in this paper this assumption can be used. A further discussion is carried out in 7.

The walking phases involving different contacts are described as follows:

- DS: Double Support, where both feet are on the ground.
- LSS: Left Single Support, where the left foot is on the ground and the right leg swings to the next support location.
- RSS: Right Single Support, as for LSS, the right foot is on the ground and the left leg is swinging.

In addition, there are also two impacts that follow each of the single support phases and precede the double support phases:

- RTD: Right Touch Down, when the left foot is in single support and the right foot strikes on the ground, we assume that when the foot of the robot touches the ground it is completely flat.
- LTD: Left Touch Down, the left foot strikes on the ground when the right foot is in single support.

To define a flat contact, it is enough to define three contact points on each of the foot, as shown in Fig 3.

Given the description of the walking phases, we illustrate in the following the dynamics equations based on few assumptions.

3.2. Dynamics

The robot is described with the generalized coordinates $\mathbf{q} \in \mathbb{R}^{n_{dof}}$, where $n_{dof} = 21$, with 15 internal DOF and 6 external DOF describing the floating base, with three translations along x, y, z and three rotations about the same axis represented with Euler angles.

The dynamics of a rigid multi-body system such as a robot can be described by the equations of motion:

$$\mathbf{H}(\mathbf{q})\ddot{\mathbf{q}} + \mathbf{C}(\mathbf{q}, \dot{\mathbf{q}}) = \boldsymbol{\tau}, \tag{1}$$

where the matrix $\mathbf{H}$ is the joint space inertia matrix, $\ddot{\mathbf{q}}$ is the joint acceleration vector, $\mathbf{C}$ the Coriolis, centrifugal and gravitational term and $\boldsymbol{\tau}$ are the joint torques. Given that the robot is a floating base system, the vector of joint torques is assumed to be:

$$\boldsymbol{\tau} = \begin{bmatrix} \mathbf{0} \\ \boldsymbol{\tau}_A \end{bmatrix}, \tag{2}$$

where $\boldsymbol{\tau}_A \in \mathbb{R}^{15}$, is the vector of active joint torques.

We introduce the following set of constraints due to contacts:

$$\mathbf{g}(\mathbf{q}) = \mathbf{0}, \tag{3}$$

Preprints (www.preprints.org) | NOT PEER-REVIEWED | Posted: 15 December 2017 doi:10.20944/preprints201712.0099.v1
Peer-reviewed version available at Appl. Sci. 2018, 8, 278; doi:10.3390/app8020278

which depend on the walking phases, as previously described.

In our formulation we assume that contacts are perfectly rigid and non-sliding and impacts are instantaneous and inelastic. Therefore, taken into account (3) into (1) we obtain:

$$\mathbf{H}(\mathbf{q})\ddot{\mathbf{q}} + \mathbf{C}(\mathbf{q}, \dot{\mathbf{q}}) = \boldsymbol{\tau} + \mathbf{G}^T\boldsymbol{\lambda}, \tag{4}$$

where $\boldsymbol{\lambda}$ is the vector of external forces due to the contacts and $\mathbf{G} == (\partial \mathbf{g}/\partial \mathbf{q})$ is the contact Jacobian.

An additional set of equations for the contact constraints is obtained by differentiation twice Eq. (3):

$$\mathbf{G}(\mathbf{q})\ddot{\mathbf{q}} + \dot{\mathbf{G}}(\mathbf{q})\dot{\mathbf{q}} = \mathbf{0}. \tag{5}$$

Combining the Eq. (4) and (5) we obtain the following system of equations for unknown $\ddot{\mathbf{q}}$ and $\boldsymbol{\lambda}$:

$$\begin{bmatrix} \mathbf{H} & \mathbf{G}^T \\ \mathbf{G} & \mathbf{0} \end{bmatrix} \begin{bmatrix} \ddot{\mathbf{q}} \\ -\boldsymbol{\lambda} \end{bmatrix} = \begin{bmatrix} \boldsymbol{\tau} - \mathbf{C} \\ -\boldsymbol{\gamma} \end{bmatrix}, \tag{6}$$

where $\boldsymbol{\gamma} = \dot{\mathbf{G}}(\mathbf{q})\dot{\mathbf{q}}$. This system describes the dynamics of the continuous phases of single and double supports, i.e. DS, LSS and RSS. In the case of DS the number of contacts is of 6, i.e. both feet have flat contacts with the ground, while in the case of LSS and RSS the number of contacts is of 3, i.e. only one foot has flat contact with the ground.

Due to the assumptions on the impacts, the dynamics describing the instantaneous change in the generalized velocities can be obtained by integrating Eq. (4) and Eq. (5) over a time singleton. The following system of equations can be written for the unknown generalized velocities after the impact $\dot{\mathbf{q}}^+$ and the impulses at each constraint $\boldsymbol{\Lambda}$:

$$\begin{bmatrix} \mathbf{H} & \mathbf{G}^T \\ \mathbf{G} & \mathbf{0} \end{bmatrix} \begin{bmatrix} \dot{\mathbf{q}}^+ \\ -\boldsymbol{\Lambda} \end{bmatrix} = \begin{bmatrix} \mathbf{H}\dot{\mathbf{q}}^- \\ \mathbf{v}^+ \end{bmatrix}, \tag{7}$$

where $\dot{\mathbf{q}}^-$ are the generalized velocities before the impact, and $\mathbf{v}^+$ the desired velocity of contact points after the impact, which is $\mathbf{0}$ due to previously described assumptions. The system as in Eq. 7 describes the dynamics of the impacts LTD and RTD as in Fig. 6.

4. Optimal Control Problem

The optimal control problem is formulated to treat the hybrid dynamic system described in the previous section, therefore it results in a multiple phases optimal control problem, where each of the phases are as described in Fig. 2.

The general formulation of a multiple phases optimal control problem can be described as follows:

$$\min_{\mathbf{x},\mathbf{u},\mathbf{p},s_0,s_1,\ldots,s_{n_{ph}}} \sum_{j=0}^{n_{ph}-1} \int_{s_j}^{s_{j+1}} \Phi_L(t, \mathbf{x}(t), \mathbf{u}(t), \mathbf{p})dt + \Phi_M(s_{j+1}, \mathbf{x}(s_{j+1}), \mathbf{p}) \tag{8}$$

subject to:

$$\begin{array}{rcl} \dot{\mathbf{x}}(t) & = & \mathbf{f}_j(t, \mathbf{x}(t), \mathbf{u}(t), \mathbf{p}), \\ & & t \in [s_j, s_{j+1}] \\ & & j = 0, \ldots, n_{ph} - 1, \\ & & s_0 = 0, s_{n_{ph}} = T \\ \mathbf{x}(s_j^+) & = & \tilde{\mathbf{J}}_j(\mathbf{x}(s_j^-), \mathbf{p}),\ j = 0, .., n_{ph} - 1 \\ g_j(t, \mathbf{x}(t), \mathbf{u}(t), \mathbf{p}) & \geq & \mathbf{0},\ t \in [s_j, s_{j+1}] \\ r^{eq}(\mathbf{x}(0), .., \mathbf{x}(T), \mathbf{p}) & = & \mathbf{0} \\ r^{ineq}(\mathbf{x}(0), .., \mathbf{x}(T), \mathbf{p}) & \geq & \mathbf{0} \end{array} \tag{9}$$

Preprints (www.preprints.org) | NOT PEER-REVIEWED | Posted: 15 December 2017 doi:10.20944/preprints201712.0099.v1

Peer-reviewed version available at Appl. Sci. 2018, 8, 278; doi:10.3390/app8020278

In the problem formulation, objective functions of Lagrangian type $\Phi_L(\cdot)$ and/or a Mayer type $\Phi_M(\cdot)$ are minimized with respect to the states $\mathbf{x}(t)$, the controls $\mathbf{u}(t)$ and the model parameters $\mathbf{p}$. These objective functions can be different for each phases, as described by the sum over the number of phases n_{ph}. The constraints of the OCP are defined in Eq. (9), where $\mathbf{f}_j(\cdot)$ is the differential equation describing the phase j, with duration of the phase j being s_j. The transition function between two consecutive phases is $\tilde{J}(\mathbf{x}(s_j^-, \mathbf{p}))$. The path constraints are represented by $g_j(\cdot)$ and $r^{eq}(\cdot)$ and $r^{ineq}(\cdot)$ are the boundary conditions and point equality and inequality constraints.

In the case of the walking problem, the number of phases is $n_{ph} = 10$, of which 7 are continuous phases and 3 are the impacts, which are modeled as phases with zero time.

4.1. States, controls and parameters

The states of the optimal control problem are the generalized positions and velocities of the robot in the case of rigid actuation:

$$\mathbf{x}(t) = \begin{bmatrix} \mathbf{q}(t) \\ \dot{\mathbf{q}}(t) \end{bmatrix} \tag{10}$$

where $\mathbf{q}, \dot{\mathbf{q}} \in \mathbb{R}^{n_{dof}}$. Which means that the right hand sides of the differential states are:

$$\dot{\mathbf{x}}(t) = \begin{bmatrix} \dot{\mathbf{q}}(t) \\ \ddot{\mathbf{q}}(t) \end{bmatrix} = \begin{bmatrix} \dot{\mathbf{q}}(t) \\ FD(\mathbf{q}, \dot{\mathbf{q}}, \boldsymbol{\tau}) \end{bmatrix}, \tag{11}$$

where $FD(\cdot)$ is a forward dynamics computation. The right hand side of each continuous phase is described by the equations as in Eq. (6) with specific sets of contacts as per Fig. 2. The transition functions $\tilde{J}(\mathbf{x}(s_j^-, \mathbf{p}))$ associated with state variable discontinuities consist in the impact dynamics equations as in Eq. (7).

The controls are represented by the active joint torques:

$$\mathbf{u}(t) = \boldsymbol{\tau}_A(t). \tag{12}$$

Therefore $\mathbf{u} \in \mathbb{R}^{15}$.

The set of parameters include the step length and the step width, expressed in [m]. The former is left free to the optimization while the latter is kept fixed to 0.14 [m] for the time being:

$$\mathbf{p} = \begin{bmatrix} p_{steplength} \\ p_{stepwidth} \end{bmatrix}. \tag{13}$$

The step width is the distance between the feet at touchdown, i.e. when both feet are on the ground and does not apply for the single support phases when one of the legs is swinging.

The duration of each phase s_j, and therefore also the total time T, is left free to the optimization to find for the best value for the specific parameters and objective functions.

4.2. Constraints

As we want to obtain feasible motions for an existing humanoid robot, boundary constraints need to be set according to the physical limits of the robot on:

- Joint angles range,
- Joint velocities,
- Torques.

Ground reaction forces and contact positions are checked according to the contact points of each phase by means of the contact points of each foot as described in Fig. 3, modeled as equality and inequality constraints. Depending on the phase, the ground reaction forces have to be positive when

Preprints (www.preprints.org) | NOT PEER-REVIEWED | Posted: 15 December 2017 doi:10.20944/preprints201712.0099.v1

Peer-reviewed version available at Appl. Sci. 2018, 8, 278; doi:10.3390/app8020278

the contact is established and the positions have to be zero on z, e.g. during RSS the right foot reaction forces have to be positive and the foot flat on the floor, while the left foot positions have to be above the floor level to avoid penetration issues.

Collision avoidance also represents a key constraint that need to be enforced in motion generation for robots. In this work it is modeled as a set of constraints based on geometric capsules, i.e. cylinders with rounded caps [29] as shown in Fig. 4. The cylinders approximate the limits of each of the links of the legs, such as the upper leg, the lower leg and the foot, for both legs. The distance $d(i,j)$ between the capsules i and j is used as constraint to avoid collision between links, i.e. $d(i,j) > 0$, where i and j are couples of different links of the two legs.

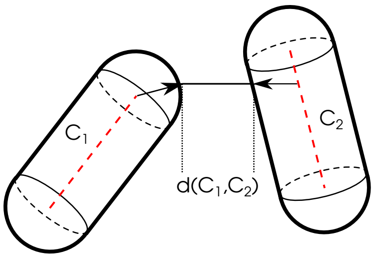

Figure 4. Collision avoidance with rounded caps. The distance between the two is calculated as d.

Orientation constraints are enforced on the feet and torso of the robot only at the start and end of the phases as equality constraints, such that after touchdown the feet are straight aligned and the torso upright with respect to the world reference frame.

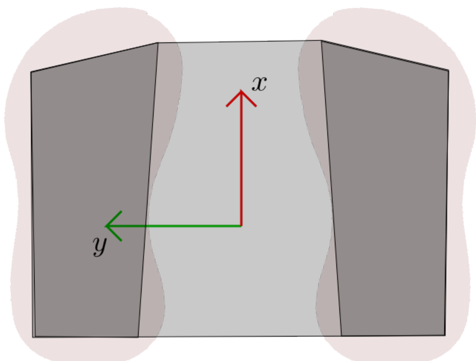

Figure 5. Approximation of the support area of the foot. The darker grey zones delimit the support areas for single support cases. The lighter grey zone changes according to the positions of the feet.

As stability criterion we use the ZMP, which we ensure lies inside the support polygon, which is approximated by a polygon that approximates the shape of the foot during single support phases and an enlarged polygon including both feet and the area between the feet during double support phases, as depicted in Fig. 5. The ZMP is computed from the ground reaction forces using the whole-body model of the robot.

Periodicity constraints are enforced on the intermediate periodic step as depicted in Fig. 2. We impose a one-step periodicity, i.e. at the end of the step the state of the robot is mirrored with respect to the beginning, meaning that left and right legs have mirrored configuration, as well as the torso, such that by mirroring the obtained periodic step we can obtain a full sequence of multiple steps. The periodicity is imposed on states $\mathbf{x}$ and controls $\mathbf{u}$.

The joint velocities are constrained to be zero at the beginning of the first phase and at the end of the last phase as equality constraints, to ensure that the motion starts from a complete stop and ends with a complete stop, i.e. $\dot{\mathbf{q}}(0) = \mathbf{0}, \dot{\mathbf{q}}(T) = \mathbf{0}$.

Preprints (www.preprints.org) | NOT PEER-REVIEWED | Posted: 15 December 2017 doi:10.20944/preprints201712.0099.v1

Peer-reviewed version available at Appl. Sci. 2018, 8, 278; doi:10.3390/app8020278

4.3. Objective functions

Different objective functions have been defined for the problem of walking, which can be combined by means of weighting factors:

- Minimization of joint torques squared, which is always included to ensure smooth torques (with small weighting factor):
$$\Phi_{\tau}(\cdot) = \mathbf{W} \cdot \mathbf{u}^T \mathbf{u}. \tag{14}$$
- Minimization of absolute mechanical work:
$$\Phi_{work}(\cdot) = \mathbf{W} \cdot \sum_{i=0}^{n_{dof}-6} \mid \dot{q}_{i-6} \cdot u_i \mid . \tag{15}$$
- Minimization of joint accelerations squared in order to obtain smooth velocity trajectories (with small weighting factor):
$$\Phi_{\ddot{q}}(\cdot) = \mathbf{W} \cdot \ddot{\mathbf{q}}^T \ddot{\mathbf{q}}. \tag{16}$$
- Torso stabilization in terms of torso movements respect to the world reference:
$$\Phi_{torso}(\cdot) = \theta_{torso} - \theta_{world}. \tag{17}$$

The matrix $\mathbf{W}$ is a weighting matrix that allows to weight differently each joint, as not all joints have equal contribution and equal order of magnitude. For the time being, the same $\mathbf{W}$ is used for all objective functions.

The reason for which the torso stabilization has been included as one of the objectives is that it has been observed that the torso performs large movements in order to compensate for the angular momentum, given that the robot does not have arms. Since the robot also has cameras on the torso, which faces to the front, it is desired that the movements of the torso with respect to the world reference are not too large, this is similar to the necessity of head stabilization in many humanoid robots.

The above listed objective functions can then be combined as one weighted objective:

$$\Phi_L(\cdot) = c_\tau \Phi_\tau + c_{work}\Phi_{work} + c_{\ddot{q}}\Phi_{\ddot{q}} + c_{torso}\Phi_{torso} \tag{18}$$

The weighting factors serve to scale the contribution of each objective but also to take into account the difference in order of magnitudes. Different combinations of the weighting factors are being explored in the next section.

5. Results

In this section we first briefly describe the software tools that have been used to achieve the results of the optimal control framework, then the numerical results are shown.

5.1. Software tools

The multiple phases optimal control problem is solved with the software package MUSCOD-II [30] of IWR (Interdisciplinary Center for Scientific Computing), Heidelberg University. The solution of the OCP is carried out using the direct multiple-shooting method as described in [31], in which controls and states are discretized. The phase times $s_{n_{ph}}$ are divided into m_{ph} intervals, over which a simple function (constant or linear) is chosen for the controls. State variables are parametrized with the multiple shooting method, which in this cases uses the same grid as the control discretization. From these two discretizations we obtain a large but structured NLP (Nonlinear Programming problem), which is solved using an adapted SQP (Sequential Quadratic Programming) method. The dynamics of the system is handled on all multiple shooting intervals in parallel to the NLP solution by means of an efficient integrator at a desired precision.

Preprints (www.preprints.org) | NOT PEER-REVIEWED | Posted: 15 December 2017 doi:10.20944/preprints201712.0099.v1

Peer-reviewed version available at Appl. Sci. 2018, 8, 278; doi:10.3390/app8020278

In this paper we choose to use piecewise constant discretization for the controls, with 50 intervals for the single support phases and 25 for the double support phases, as they are usually shorter than the single support phases. The number of shooting intervals is chosen identical to the control intervals.

The dynamics quantities are computed using the Rigid Body Dynamics Library (RBDL) [32], which allows for the computation of forward dynamics with contacts as well as impact dynamics.

5.2. Numerical results

We generated different motions with combinations of different optimality criteria. In particular we have used the following combinations, which are summarized as in Table 1:

1. Minimization of joint torques, with a small weight on minimization of joint accelerations.
2. Minimization of joint torques and torso stabilization, with a small weight on minimization of joint accelerations.
3. Minimization of absolute work, with a small weight on minimization of joint torques and joint accelerations.
4. Minimization of absolute work and torso stabilization, with a small weight on minimization of joint torques and joint accelerations.

Table 1. Combination of objective functions. Minimization of torques and joint accelerations are always included with small weighting factors to ensure smooth trajectories.

Objectives	$\Phi_{\tau}(\cdot)$	$\Phi_{work}(\cdot)$	$\Phi_{\ddot{q}}(\cdot)$	$\Phi_{torso}(\cdot)$
1	1	0	10^{-4}	0
2	1	0	10^{-4}	10
3	10^{-4}	1	10^{-4}	0
4	10^{-4}	1	10^{-4}	10

The computations have been carried out using MUSCOD-II and RBDL on a standard desktop pc with i7 CPU running at 3.60 GHz with 8 cores. For the whole sequence to be computed the average time is about 12-15 hours, due to the chosen number of intervals.

As setting the initial guess all to zeros is not a realistic choice for such a large and complex nonlinear optimization problem, the initial guess is generated from a sequence of walking motion obtained with the reduced models from our previous works and set as the same for all combinations of objectives considered. We cannot ensure that the obtained results are completely independent from the initial guess, but the outcomes have shown that the resulting motions show differences with respect to the ones generated with reduced models. This can be seen in a more intuitive way from the example of a motion sequence of a single step shown in Fig. 6. The first sequence is a motion generated with the 3D Linear Inverted Pendulum Model (LIPM), in this case the whole-body motion was obtained applying inverse kinematics to given center of mass and feet trajectories from a pattern generator. In order to generate feasible trajectories, the orientations of feet and torso have been constrained with respect to the world reference frame. In contrast to the first sequence, the second sequence, which is generated with optimal control with minimization of torques (case 1 in Table 1), shows a clear change in the orientation of both torso and swing foot. As also discussed in section 4, the stabilization of the torso might be a desired feature, therefore in the third sequence it is possible to see how the torso is stabilized using the set of objectives as per case 2 in Table 1.

In order to show the results in a more consistent way, the intermediate periodic step has been concatenated into 9 steps, resulting in a sequence of a total of 11 steps for each of the cases as listed in Table 1. The resulting CoM trajectories are shown in Fig. 7 and the whole-body joint trajectories are shown in Fig. 8. The effect of the torso stabilization can be seen in a clear way in Fig. 9, which shows the orientation of the torso with respect to the world reference frame during the whole walking sequence.

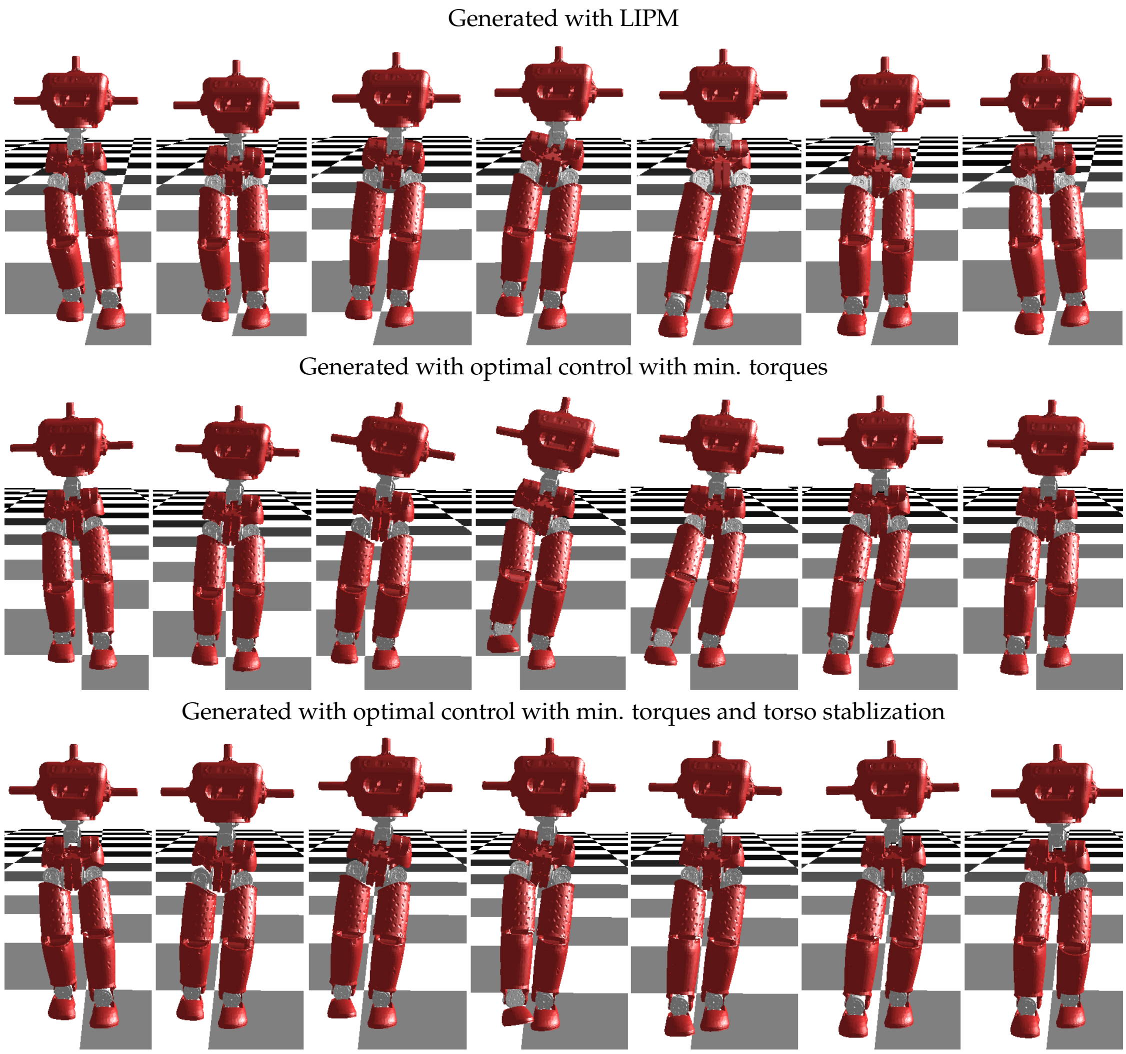

Figure 6. Example sequences of one step motions from using the reduced model, the whole-body model minimizing torques and the whole-body model with torso stabilization.

From the results, with respect to methods based on reduced models, a major difference that can be observed is the variation in height of the CoM, which is usually kept fixed due to the linearization of the ZMP equations. Using optimal control instead, we have not introduced such constraint, and as we can observe from Fig. 8 the knee joint has big variations and reaches also completely stretched configurations. The CoM height variation presents however spikes when switching to the next step, these spikes are due to the impacts which are set with zero velocity as per our assumptions in Sec. 3. In future work, they could be reduced by minimizing the impact forces. We can also observe that despite the CoM projection on the ground (xy plane) is still very similar to what is usually obtained with the reduced models as in [8,18]. This is mainly due to mechanical design and restrictions of the robot itself, such as the rigid flat feet and also the missing arms. The reason for which without torso stabilization the robot swings the torso is to compensate for the angular momentum. If the robot had arms they could be used to achieve angular momentum compensation, but it is not the case for HeiCub. As a matter of fact, we can observe from Fig. 6 that when the torso stabilization is introduced, the robot takes steps with smaller step width during swing phase with respect to the case when there is no torso stabilization. From Fig. 7 and 8 we can also observe the differences between the motion obtained with minimization of torques and absolute work, where the latter shows a more constant variation in the CoM trajectory and the legs are turned inwards.

Preprints (www.preprints.org) | NOT PEER-REVIEWED | Posted: 15 December 2017 doi:10.20944/preprints201712.0099.v1
Peer-reviewed version available at Appl. Sci. 2018, 8, 278; doi:10.3390/app8020278

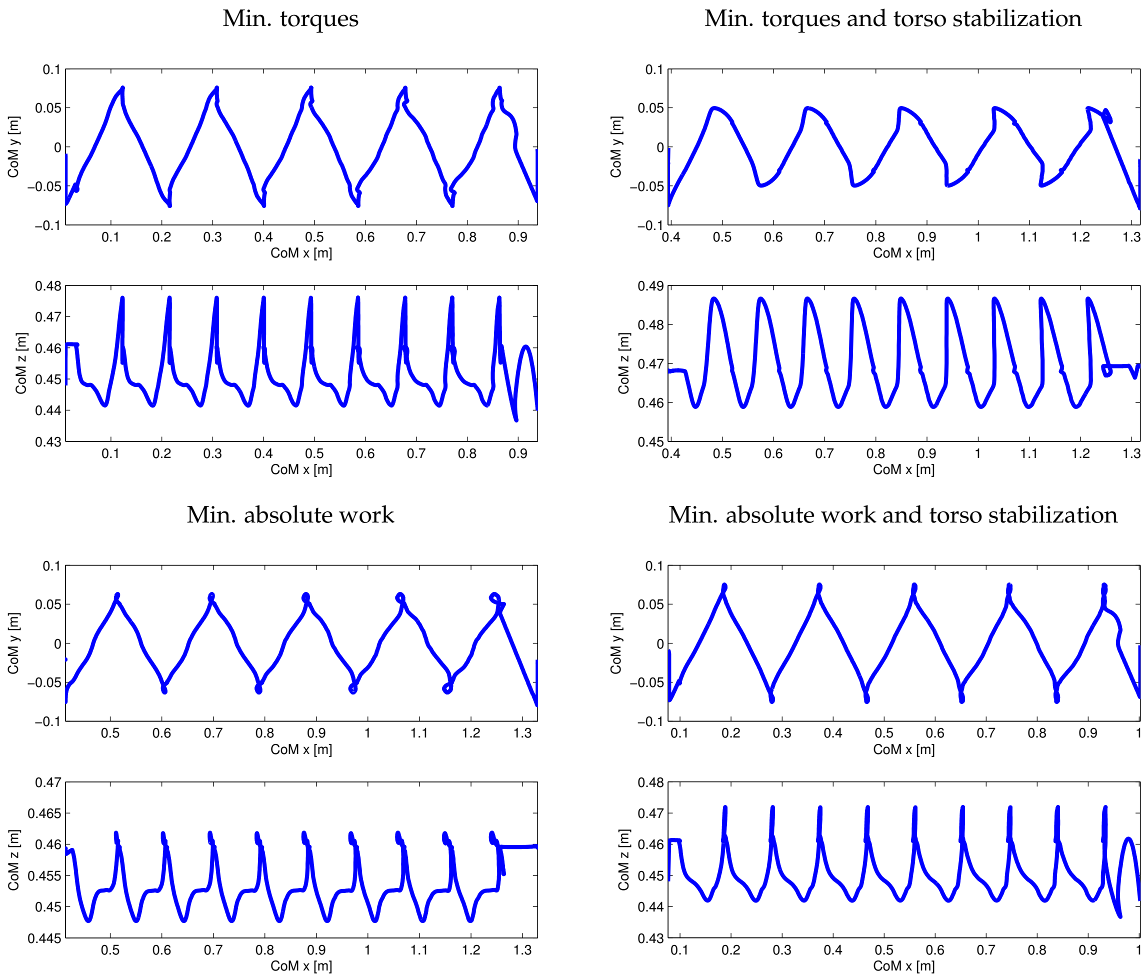

Figure 7. Center of mass trajectories of a full sequence with 9 periodic steps combinations of objectives as in Table 1.

6. Experimental validation

In order to test the obtained motion sequences on the robot, the periodic step has been concatenated to obtain a longer sequence of walking of 9 periodic steps. The motions are executed on the robot by means of position control in open loop with closed loop joint angle tracking. This choice is due to the fact that torque control for walking on the iCub family robots still cannot ensure good torque tracking, as the robot does not have joint torque sensors, the torques are estimated via force torque sensors that often incur in saturation issues at impacts and cannot therefore ensure precise torque tracking for motions such as walking.

The trajectories obtained from the optimal control framework are discretized as per the discretization grid chosen for MUSCOD-II, which does not correspond to the thread rate required by the robot controller. Due to the choice of letting the time free in the optimization, it is not possible to choose a discretization grid that corresponds exactly to the thread rate. Also, the number of shooting nodes would be too high for the problem to be solvable in a reasonable time. Therefore, all the trajectories have been interpolated with a spline interpolation in order to obtain the correct number of samples required by the robot controller. Furthermore, it is to be noted that currently on the robot there is no proper implementation of the floating base estimation, therefore the sliding effects that might occur during the execution of the motions are not compensated. The CoM trajectories of the robot are obtained with the computed floating based and the joint angle trajectories from the encoders.

Preprints (www.preprints.org) | NOT PEER-REVIEWED | Posted: 15 December 2017 doi:10.20944/preprints201712.0099.v1

Peer-reviewed version available at *Appl. Sci.* **2018**, *8*, 278; doi:10.3390/app8020278

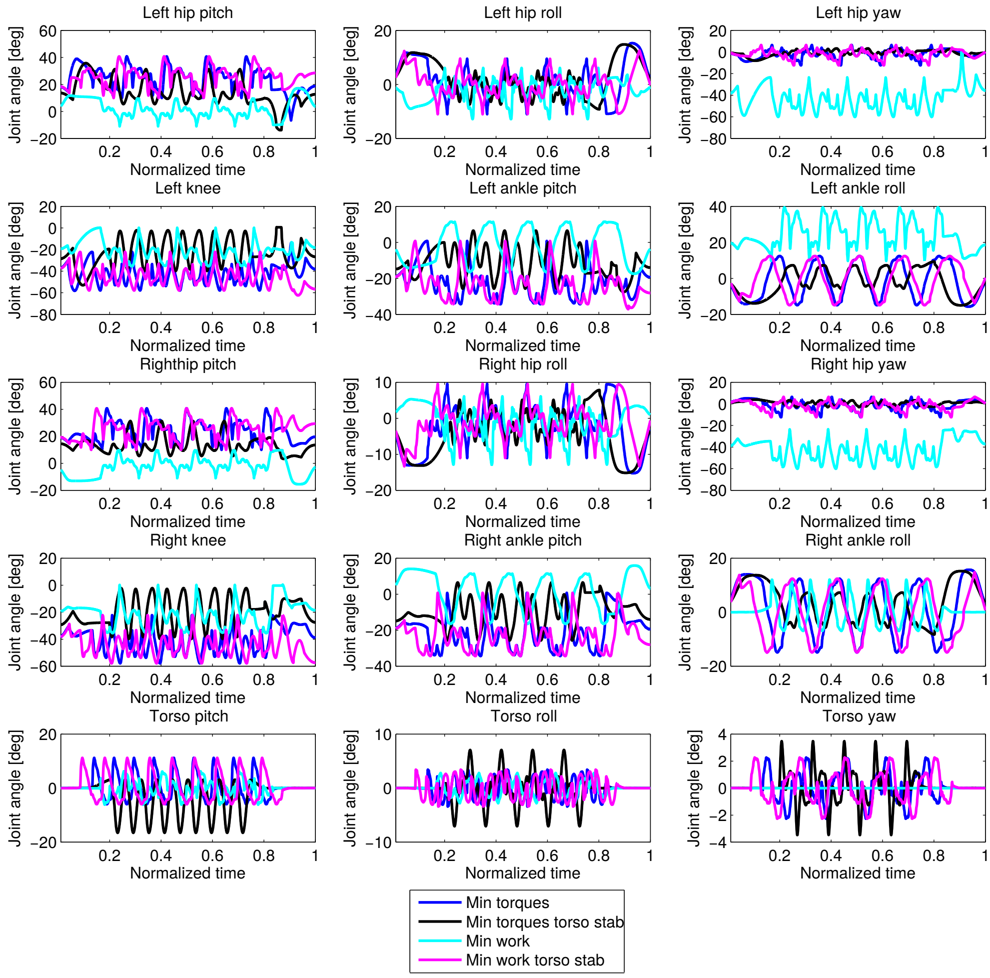

Figure 8. Joint angle trajectories of all the 15 DOF of the robot, obtained for the 4 combinations of objective functions. Time is normalized for all trajectories for comparison reasons. It is to be noted that torso stabilization does not mean reduction of the movements of the torso joints, but the orientation w.r.t. the world reference.

The robot has executed all four obtained motions, proving the feasibility of the motions and of the periodicity constraints. We can see the resulting CoM trajectories in red in Fig. 10. We can observe from the results that the CoM trajectories could be followed closely by the robot, however when the torso stabilization is not included, a bigger deviation can be observed in the height of the CoM trajectory in correspondence of the spikes, this is due to the impact forces as mentioned in the previous section. It seems however that the introduction of torso stabilization has a damping effect on the error when executed on the robot.

To compare in a more systematic way the outcomes of the optimal control framework on the robot with the results obtained in our previous works with reduced models, we computed the Key Performance Indicators, which are illustrated in details in the following section.

Preprints (www.preprints.org) | NOT PEER-REVIEWED | Posted: 15 December 2017 doi:10.20944/preprints201712.0099.v1

Peer-reviewed version available at Appl. Sci. 2018, 8, 278; doi:10.3390/app8020278

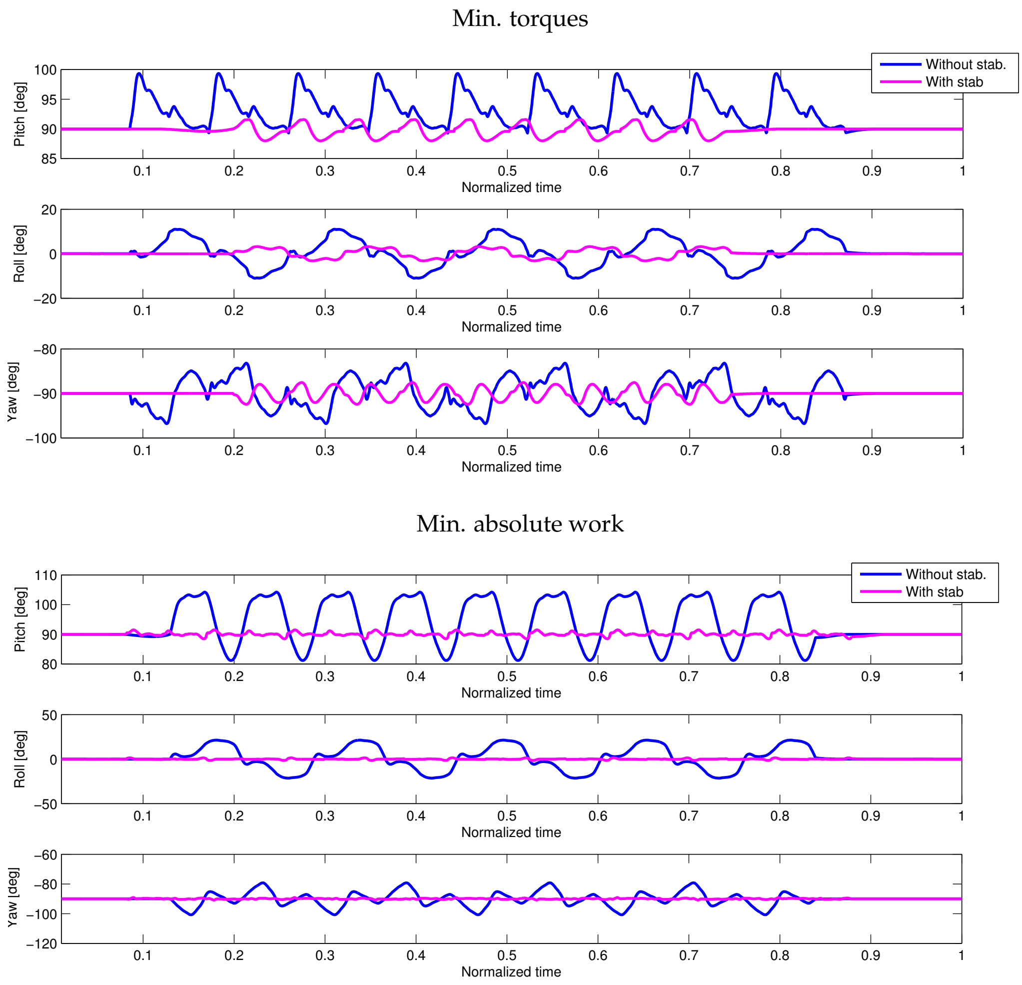

Figure 9. Torso orientation trajectories for the two cases of minimization of torques and absolute work. The orientation is expressed with respect to the world reference frame, the nominal reference (torso upright) is [90,0,-90]. Time is normalized for all trajectories for comparison reasons.

6.1. Key Performance Indicators (KPI)

The Key Performance Indicators (KPIs) are a series of indicators developed in the European Project KoroiBot [1] designed to compare the performances of different methods applied on humanoid robots. These indicators are meant to compare the walking capabilities of the same humanoid robot with different control approaches and/or methodologies, and not to compare different robots, as it is highly difficult to compare robots that are very different in size and mechanical structure.

For the HeiCub a subset of the KPIs have been defined in our previous works [8,18]. In the following we give a brief explanation of the measured indicators, which were chosen based on quantities that are measurable from the robot sensors:

- **Walking velocity** v_{max}
  The maximum achieved walking velocity, in the case of motions generated with optimal control this corresponds to the velocity of the resulting sequence.

1 http://www.koroibot.eu

Preprints (www.preprints.org) | NOT PEER-REVIEWED | Posted: 15 December 2017 doi:10.20944/preprints201712.0099.v1

Peer-reviewed version available at Appl. Sci. 2018, 8, 278; doi:10.3390/app8020278

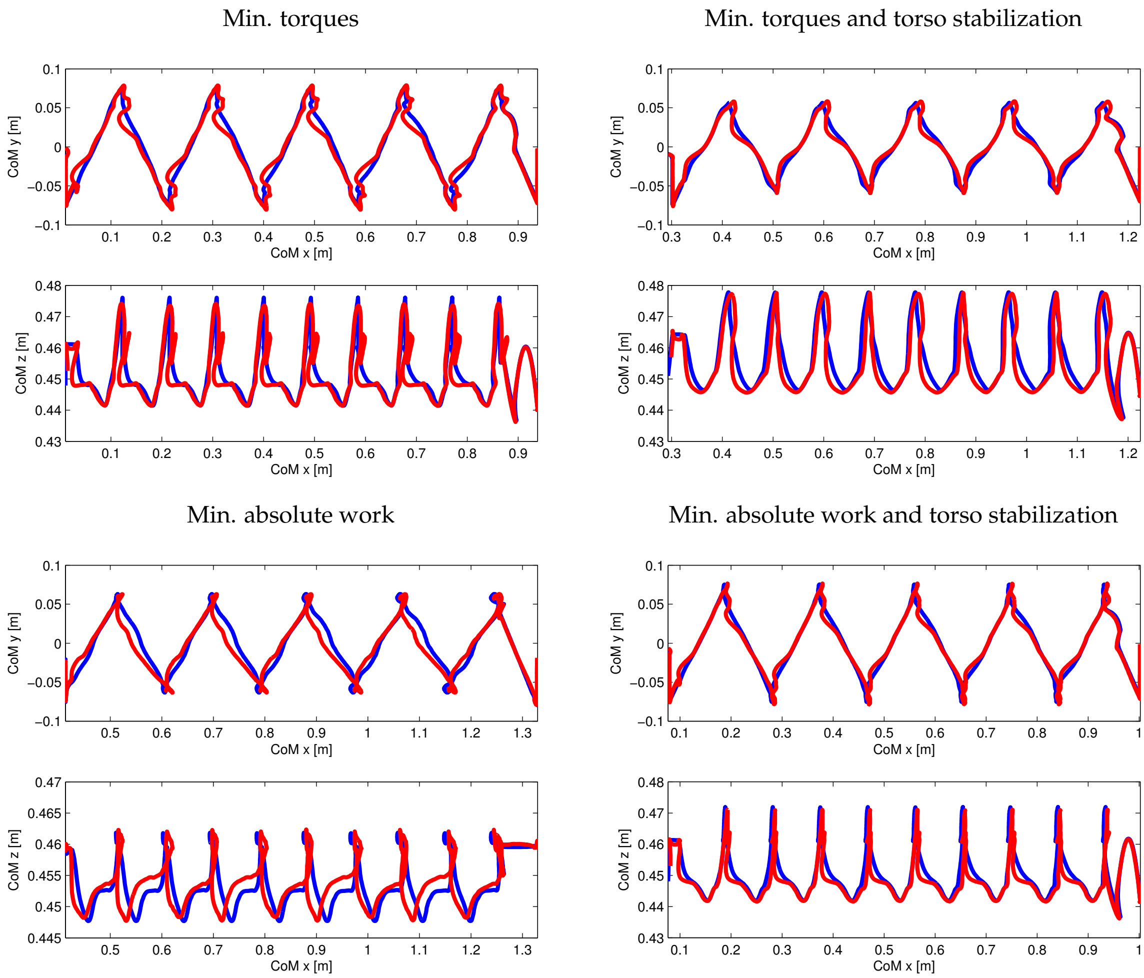

Figure 10. Center of mass trajectories obtained on the robot (in red) with all four combinations of objective functions as in Table 1.

- **Walking timings** t^{ss}/t^{ds} and step period
  Single and double support times of a single step, which whole durations is indicated as the step period. In the case of optimal control, we consider the timings of the periodic step.
- **Cost of Transport**

$$\mathbf{E}_{CT} = \frac{\sum_{m=1}^{M} \int_{t_0}^{t_f} I_m(t) V_m(t) dt}{m_{robot} g \cdot d} \tag{19}$$

  The Cost of Transport is defined as a unitless quantity, where M is the total number of motors, I_m and V_m are the current and voltage measurements of the motor m, m_{robot} is the mass of the robot and d is the travelled distance.
- **Froude number**

$$Fr = v_{max} / \sqrt{g \cdot h}, \text{ for } h = l_{leg} \tag{20}$$

  where l_{leg} is the robot leg length. The Froude number is a dimensionless number used in fluid mechanics to characterize the resistance of an object moving through water. Alexander used it to characterize animal locomotion, given the that also legged locomotion is a dynamic motion in gravity [33]. A given Froude number can be assigned to a certain walking style. Running, for example, starts at a Froude number of approximately 1.0

Preprints (www.preprints.org) | NOT PEER-REVIEWED | Posted: 15 December 2017 doi:10.20944/preprints201712.0099.v1

Peer-reviewed version available at Appl. Sci. 2018, 8, 278; doi:10.3390/app8020278

- **Precision of task execution**:
  Expressed in terms of tracking errors. The root mean square error is computed by summing the squared difference between the measurement and the desired position over all points of the whole trajectory.

Table 2. Key Performance Indicators (KPIs) measured for all 4 combinations of objective functions, in comparison with results with reduced models. The support times and step period are referred to the ones of the periodic step.

KPIs	Cart-Table	NMPC (LIPM)	Min torques	Min torques & torso stab.	Min work	Min work & torso stab.
v_{max} [m/s]	0.037	0.065	0.053	0.079	0.043	0.053
t^{ss}/t^{ds} [m/s]	1.5 / 1.0	0.6 / 0.6	1.06 / 0.98	0.7 / 0.37	1.06 / 1	0.8 / 0.8
step period [s]	2.5	1.2	2.04	1.07	2.06	1.6
Cost of Transport	4.27	2.99	2.69	1.97	3.32	3.09
Froude Number	0.017	0.029	0.024	0.035	0.019	0.024
Joint error [deg]	1.45	1.21	1.27	1.29	1.11	0.9
CoM error [cm]	0.61	0.44	0.29	0.31	0.39	0.29

The KPIs computed for each of the combinations of objective functions as in Table 1 are reported in Table 2. In this table we report also the ones obtained from previous works [8,18] for comparison reasons. As we can see from this table, the cost of transport could be reduced with the minimization of torques, while the minimization of mechanical work does not show significant improvements in these indicators with respect to the reduced models. When stabilizing the torso, the motion generated using optimal control outperforms the reduced model in walking speed as the double support time is much shorter, as a matter of fact also cost of transport and Froude number are better in this case with respect to the other cases. In our objective functions we did not aim at maximizing walking velocity but rather left the optimization to find the best solution for the given objective, therefore it was not expected that the walking speed would necessarily outperform the reduced models. The results however show that the robot can achieve faster walking within its physical limitations, which was not possible with the reduced models.

7. Discussion & Conclusions

In this paper, we have presented the first results of optimal control methods applied to whole-body models of an iCub robot for generating walking motions. We have also described the underlying framework and model in much detail. In contrast to other approaches to motion generation, optimization is an all at once approach that determines all characteristics of a motion simultaneously to optimize a chosen performance criterion called the objective or cost function, and to satisfy all important constraints related to the robot and the task description. For this research, we have focused on the HeiCub robot which is a reduced version of the iCub with no head and no arms, but the same approach could be applied to the full iCub by just using the corresponding model which is also available.

In our previous research, the HeiCub had already achieved walking, using methods based on reduced models such as the LIPM and the table cart, and these approaches also have been transferred to the full iCub. These experiences also allowed us to identify parameters and physical constraints that were now included in the optimal control problem formulations. Even though the simplified approaches allowed to generate a variety of walking motions on level ground in different directions (forward, backward, sidewards), and up and down stairs and slopes, the motions showed some of the typical characteristics of walking based on simplified models, e.g. keeping the pelvis at (nearly) constant height, resulting in a less dynamic appearance of the gait. In addition, the weight distribution of the HeiCub robot violates some of the center of mass assumptions taken for the simple models (see Sec. 2), because its legs are comparatively heavy. Walking generation methods taking into account the

Preprints (www.preprints.org) | NOT PEER-REVIEWED | Posted: 15 December 2017 doi:10.20944/preprints201712.0099.v1

Peer-reviewed version available at Appl. Sci. 2018, 8, 278; doi:10.3390/app8020278

precise mass distribution of the robot therefore seemed to be very promising to generate more suitable motions on the robot, especially since we already had positive experiences with such methods with generating squatting motions and simple push recovery steps for the same robot [34,35] as well as complex walking motions for other humanoid robots, such as HRP-2 [12].

The results of this first optimization study are very encouraging. We have shown that

- it is possible to formulate optimal control problems for the iCub / HeiCub robots that allow to simultaneously generate periodic walking motions as well as the necessary starting and stopping steps that take the robot from standing position to the periodic cycle as well as from back to standing position. So far, only single starting and stopping steps have been included in the formulation, but it is straightforward to extend this to multiple steps, which may be required for faster walking.
- different objective functions result in visibly different walking styles for the robot. In particular we have compared a minimization of torques squared and of absolute mechanical work, in both cases with and without a combined term on torso stabilization. A very small term on joint accelerations was present in all objective functions. Further objective functions are subject of current research. The fact that we are able to generate walking in different styles in an automated way already presents a significant difference to the classical walking generation methods using the simple models for which all outcomes look very similar.
- the resulting motions are still not close to a biological motion, but they have made a significant progress in the right direction. In particular, the motions show variations in the height of the CoM. See the discussion below for making optimized walking motions more biological or ˋhuman-likeˊ.

As discussed in the introduction, optimization can be a very helpful tool to bring humanoid robots to their technical limits, i.e. to make the most out of given robot hardware. This requires that suitable optimization criteria targeting an improvement of performance are used which has not been done so far in this study. In current research, we are also looking at step length, step frequency and walking speed maximization. The objective functions used in this study targeted the smoothness of motions as well as measures of efficiency. We are also interested in using human-inspired criteria for generating humanoid motions. For this, we can rely on results of inverse optimal control studies which identify criteria underlying human motions from motion capture data. These criteria can then be applied to humanoid models in optimal control problem formulations as the one presented in this paper. We have demonstrated a similar approach based on simpler template models of human and humanoid walking in [16], also for the HeiCub, but it would be new to apply this concept of transferring bio-inspired optimization criteria to whole-body models of the HeiCub robot.

There are several characteristics of the robot and its inherent control approaches that limit the performance. The fact that the robot has no arms and all counteraction to the lower limb angular momentum has to be done by the torso, already prevents it from acting in a fully human-like manner. While humans exhibit a strongly stabilized head and torso while walking forward on flat ground, such a criterion induces strong limitations to the motion if no actions of arms are possible. In this context, also the extension of the work to the full iCub model would be interesting to see how the arms are used for angular momentum compensation.

As discussed before, the HeiCub and iCub robots also have several limitations in the joint angles, the angular velocities and the joint torques, that prevent it from coming close to human performance. In addition, the current foot shape and controllers impose that the robot - as most contemporary robots - walks with flat feet and can not e.g. have heel only or toe only contact as humans can, resulting in limited step lengths and step heights (the latter on stairs). The optimal control approach presented in this paper could also serve to generate walking motions with partial or more flexible foot contact, as soon as the hardware allows it. While optimization can help to exploit the capabilities of the robot hardware it is best to simultaneously also improve the hardware to have an overall performance improvement.

As mentioned in Sec. 2, the robot is equipped with Series Elastic Actuators. The model of the robot with reduced number of DOF but including elasticity has been used in optimal control frameworks for the generation of squat and push recovery motions [34,35], the current framework for walking will be extended to include also the elasticity of the elastic actuators, which will be mounted for the experimental validations. The optimal control problem including elasticity is a larger nonlinear problem with respect to the one described in this work, which will require longer computation times. On the hardware side, a proper control for the SEA need to be implemented.

In addition to the extensions already discussed, future work o whole-body optimal control of the HeiCub robot will also include more complex walking scenarios like stairs and slopes for which the approach based on simple models is even further from the real behaviour than for motion on flat ground an for which many details of the motion such as the foot trajectories in the air had to be inserted manually. We expect that for these motions the gain in performance and walking quality by the whole-body optimal control approach will be more significant than for walking.

The computation times for the method presented here, are very long for multiple reasons. First, it should be noted that the whole-body dynamic equations for a complex multi-phase system have to be solved (and derivatives have to be computed) precisely in every optimization step. Second, the discretization chosen for the controls and the multiple shooting intervals in the present study is very accurate, and from the optimal control perspective a much coarser grid would be possible without any problem. This was done in the attempt to get closer to the robots control intervals, but could also be solved by means of interpolation in the interest of a higher efficiency. But what is most important is that it can be avoided to solve such optimal control problems online each time the robot has to perform a motion. In previous research, we developed an approach based on a combination of optimal control with movement primitives [15]. In this method, optimal control serves to generate multiple training data in an offline process on the basis of which movement primitives are learned. This takes some time, but is not time-critical and only has to be done once for a class of motions. New versatile motions can the be efficiently generated online, just using the movement primitives without the need to solve any optimal control problems. As it has been demonstrated in the case of another robot, the resulting motions are anyway close to optimal and dynamic feasibility and work well on the real system. We therefore expect this to be a very interesting approach for the iCub / HeiCub robot which makes this a very important argument to further explore whole-body optimal control in the context of bio-inspired walking generation for these robots.

Acknowledgments: The work carried out in this paper was funded by the Heidelberg Graduate School of Mathematical and Computational Methods for the Sciences (HGS MathComp), founded by DFG grant GSC 220 in the German Universities Excellence Initiative.

This work is based on work that was carried out for the European Project KoroiBot concluded in September 2016, which received funding from the European Union Seventh Framework Programme (FP7/2013) under the grant agreement n. 611909.

We wish to thank the Simulation and Optimization group of H. G. Bock at the Heidelberg University for providing the optimal control code MUSCOD.

Author Contributions: Yue Hu and Katja Mombaur jointly planned and designed the study and contributed to analyzing the results and writing the paper. Yue Hu has carried out the computations and the experiments.

Conflicts of Interest: The authors declare no conflict of interest. The funding sponsors had no role in the design of the study; in the collection, analyses, or interpretation of data; in the writing of the manuscript, and in the decision to publish the results.

References

1. Vukobratović, M.; Borovac, B. Zero-moment point—thirty five years of its life. *International Journal of Humanoid Robotics* **2004**, *1*, 157–173.
2. Mukovskiy, A.; Vassallo, C.; Naveau, M.; Stasse, O.; Soueres, P.; Giese, M.A. Adaptive synthesis of dynamically feasible full-body movements for the humanoid robot HRP-2 by flexible combination of learned dynamic movement primitives. *Robotics and Autonomous Systems* **2017**, *91*, 270–283.

3. Ishiguro, Y.; Kojima, K.; Sugai, F.; Nozawa, S.; Kakiuchi, Y.; Okada, K.; Inaba, M. Bipedal Oriented Whole Body Master-Slave System for Dynamic Secured Locomotion with LIP Safety Constraints. IEEE International Conference on Intelligent Robots and Systems (IROS). IEEE, 2017, pp. 376–382.
4. Kajita, S.; Kanehiro, F.; Kaneko, K.; Fujiwara, K.; Yokoi, K.; Hirukawa, H. A Realtime Pattern Generator for Biped Walking. IEEE International Conference on Robotics and Automation (ICRA). IEEE, 2002, pp. 31–37.
5. Kajita, S.; Kanehiro, F.; Kaneko, K.; Fujiwara, K.; Harada, K.; Yokoi, K.; Hirukawa, H. Biped walking pattern generation by using preview control of zero-moment point. IEEE International Conference on Robotics and Automation (ICRA). IEEE, 2003, Vol. 2, pp. 1620–1626.
6. Naveau, M.; Kudruss, M.; Stasse, O.; Kirches, C.; Mombaur, K.; Souères, P. A reactive walking pattern generator based on nonlinear model predictive control. *IEEE Robotics and Automation Letters* **2017**, *2*, 10–17.
7. Li, Z.; Tsagarakis, N.G.; Caldwell, D.G. Walking trajectory generation for humanoid robots with compliant joints: Experimentation with COMAN humanoid. IEEE International Conference on Robotics and Automation (ICRA). IEEE, 2012, pp. 836–841.
8. Hu, Y.; Eljaik, J.; Stein, K.; Nori, F.; Mombaur, K. Walking of the iCub humanoid robot: implementation and performance analysis. *IEEE-RAS International Conference on Humanoid Robots (Humanoids)* **2016**, pp. 690–696.
9. Lengagne, S.; Vaillant, J.; Yoshida, E.; Kheddar, A. Generation of whole-body optimal dynamic multi-contact motions. *The International Journal of Robotics Research* **2013**, *32*, 1104–1119.
10. Miossec, S.; Yokoi, K.; Kheddar, A. Development of a software for motion optimization of robots - Application to the kick motion of the HRP-2 robot. IEEE International Conference on Robotics and Automation (ICRA), 2006, pp. 299–304.
11. Suleiman, W.; Yoshida, E.; Laumond, J.P.; Monin, A. On humanoid motion optimization. IEEE-RAS International Conference on Humanoid Robots (Humanoids), 2007, pp. 180–187.
12. Koch, K.H.; Mombaur, K.; Souères, P. Optimization-based walking generation for humanoids. IFAC-SYROCO 2012. Elsevier, 2012, Vol. 45, pp. 498–504.
13. Koch, K.H.; Mombaur, K.; Souères, P. Studying the Effect of Different Optimization Criteria on Humanoid Walking Motions. In *Simulation, Modeling, and Programming for Autonomous Robots*; Noda, I.; Ando, N.; Brugali, D.; Kuffner, J.J., Eds.; Springer Berlin Heidelberg, 2012; Vol. 7628, *Lecture Notes in Computer Science*, pp. 221–236.
14. Koch, K.H.; Mombaur, K.; Souères, P.; Stasse, O. Optimization based exploitation of the ankle elasticity of HRP-2 for overstepping large obstacles. IEEE/RAS International Conference on Humanoid Robots (Humanoids 2014), 2014, pp. 733–740.
15. Clever, D.; Harant, M.; Mombaur, K.; Naveau, M.; Stasse, O.; Endres, D. Cocomopl: A novel approach for humanoid walking generation combining optimal control, movement primitives and learning and its transfer to the real robot HRP-2. *IEEE Robotics and Automation Letters* **2017**, *2*, 977–984.
16. Clever, D.; Mombaur, K.D. An Inverse Optimal Control Approach for the Transfer of Human Walking Motions in Constrained Environment to Humanoid Robots. Robotics: Science and Systems, 2016.
17. Metta, G.; Natale, L.; Nori, F.; Sandini, G.; Vernon, D.; Fadiga, L.; Von Hofsten, C.; Rosander, K.; Lopes, M.; Santos-Victor, J.; others. The iCub humanoid robot: An open-systems platform for research in cognitive development. *Neural Networks* **2010**, *23*, 1125–1134.
18. Stein, K.; Hu, Y.; Kudruss, M.; Naveau, M.; Mombaur, K. Closed loop control of walking motions with adaptive choice of directions for the iCub humanoid robot. IEEE International Conference on Humanoid Robots (Humanoids), 2017 - to appear.
19. Tikhanoff, V.; Pattacini, U.; Natale, L.; Metta, G. Exploring affordances and tool use on the iCub. IEEE-RAS International Conference on Humanoid Robots (Humanoids). IEEE, 2013, pp. 130–137.
20. Mar, T.; Tikhanoff, V.; Metta, G.; Natale, L. Self-supervised learning of grasp dependent tool affordances on the iCub Humanoid robot. IEEE International Conference on Robotics and Automation (ICRA). IEEE, 2015, pp. 3200–3206.
21. Nori, F.; Traversaro, S.; Eljaik, J.; Romano, F.; Del Prete, A.; Pucci, D. iCub whole-body control through force regulation on rigid non-coplanar contacts. *Frontiers in Robotics and AI* **2015**, *2*, 6.
22. Parmiggiani, A.; Metta, G.; Tsagarakis, N. The mechatronic design of the new legs of the iCub robot. IEEE-RAS International Conference on Humanoid Robots (Humanoids). IEEE, 2012, pp. 481–486.

23. Colasanto, L.; Tsagarakis, N.; Caldwell, D. A Compact Model for the Compliant Humanoid Robot COMAN. *IEEE International Conference on Biomedical Robotics and Biomechatronics* **2012**, pp. 688–694.
24. Dallali, H.; Kormushev, P.; Li, Z.; Caldwell, D. On Global Optimization of Walking Gaits for the Compliant Humanoid Robot, COMAN Using Reinforcement Learning. *Cybernetics and Information Technologies* **2012**, *12*, 39–52.
25. Moro, F.; Tsagarakis, N.; Caldwell, D. Walking in the resonance with COMAN robot with trajectories based on human kinematic motion primitives (kMPs). *Autonmous Robot* **2013**.
26. N.G. Tsagarakis, M. Laffranchi, B.V.; Caldwell, D.G. A Compact Soft Actuator Unit for Small Scale Human Friendly Robots. *International Conference on Robotics and Automation (ICRA)* **2009**, pp. 4356–4362.
27. Felis, M.; Mombaur, K.D.; Berthoz, A. An Optimal Control Approach to Reconstruct Human Gait Dynamics from Kinematic Data. *IEEE-RAS 15th International Conference on Humanoid Robots (Humanoids)* **2015**.
28. Hu, Y.; Mombaur, K. Analysis of human leg joints compliance in different walking scenarios with an optimal control approach. 6th IFAC International Workshop on Periodic Control Systems (PSYCO 2016), 2016, Vol. 49, pp. 99–106.
29. Ketchel, J.; Larochelle, P. Collision detection of cylindrical rigid bodies for motion planning. IEEE International Conference on Robotics and Automation (ICRA). IEEE, 2006, pp. 1530–1535.
30. Leinweber, D.; Bauer, I.; Bock, H.; Schloeder, J. An efficient multiple shooting based reduced SQP strategy for large-scale dynamic process optimization. Part I: Theoretical aspects. *Computers and Chemical Engineering* **2003**, *27*, 157–166.
31. Bock, H.; Plitt, K. A multiple shooting algorithm for direct solution of optimal control problems; Pergamon Press, 1984; pp. 243–247.
32. Felis, M.L. RBDL: an efficient rigid-body dynamics library using recursive algorithms. *Autonomous Robots* **2016**, pp. 1–17.
33. Alexander, R.M. *Principles of animal locomotion*; Princeton University Press, 2003.
34. Hu, Y.; Nori, F.; Mombaur, K. Squat Motion Generation for the Humanoid Robot iCub with Series Elastic Actuators. IEEE RAS & EMBS International Conference on Biomedical Robotics and Biomechatronics (BioRob). IEEE, 2016, pp. 207–212.
35. Hu, Y.; Mombaur, K. Optimal Control Based Push recovery Strategy for the humanoid robot iCub with Series Elastic Actuators. IEEE/RSJ International Conference on Intelligent Robots and Systems (IROS). IEEE, 2017, pp. 5842–5852.